The Structure of Ice-Ih

W. F. KUHS AND M. S. LEHMANN

Institut Laue–Langevin, 156X 38042 Grenoble Cedex, France

1. Introduction

Frozen water, in all its forms ranging from snowflakes to icebergs, has intrigued scientists for many centuries. Already Kepler [1] had speculated on the hexagonal shape of snowflakes, wondering what were the forces that transformed round droplets of water into the beautiful stars that he saw in falling snow. Although he did not resort to an atomic picture, he used a concept with formation by the cold of very small, identical particles, which would grow from an octahedral origin. There would thus be three orthogonal growth directions, leading to the formation of six branches in the star, and a hexagon could then form by a flattening of the star along one of the three-fold axes. Kepler discussed the form of different natural objects, ranging from honeycombs over pomegranates to different crystal forms, and he ended by proposing that different fluids would have in-built abilities that would lead to different forms when frozen.

Since then scientists have been equipped with a multitude of tools that allow them to go well beyond visual observation and speculation in the study of nature, but water in all its forms has always been a subject of interest. In this paper we shall deal with one small domain, namely the structure of ice-Ih. Methods of structure analysis originated in the first quarter of this century. Again ice was among the first compounds to be looked at with X-rays, and when neutron scattering became viable a powder spectrum of ice was among the first to be recorded.

Over the years methods of measurement and interpretation have developed, and at regular intervals ice has been studied, leading to a more and more precise and detailed picture of the atomic distribution. We shall report on this, and we shall also go on to discuss diffraction measurements, which have aimed at clarifying the pattern of disorder in ice.

Structural information is not only concerned with the atomic locations, but also with the interatomic arrangement, and this can be inferred from spectroscopic methods. In this review we have therefore also tried to extract what can be learned about distances and motions from spectroscopy, and to what extent there is agreement between the data obtained by the different methods.

Finally, theory should not be forgotten, so apart from the interpretations of observations given when needed, we report on the progress made in understanding the crystal structure with the aid of theoretical computational chemical methods.

The structure of ice-Ih seems, at first sight, a very limited topic. However, the literature on the subject is large, so to keep within a reasonable size the selection has been rather restrictive. We hope nevertheless that although only indicating the tip of the iceberg, we succeed in conveying the many exciting aspects of hexagonal ice.

2. Crystallographic studies

Ice-Ih is one of the most thoroughly disordered crystalline materials. The high translational symmetry is not retained at the level of the crystallographic unit cell. The symmetry elements of the crystallographic space group act only on the time- and space-averaged atomic densities, and there is no doubt that in this sense the symmetry in ice-Ih is very high indeed. In crystallographic studies sampling is over the instantaneous configurations in time and space provided that the interaction time of the radiation is short compared to the atomic motion and provided that the coherence length of the radiation is shorter than the size of the coherently scattering sample. Both conditions are in general fulfilled for studies on ice-Ih single crystals or powders with neutron or X-ray radiation. However, the atomic configurations in one specific unit cell do not obey the symmetry governing the time and space average. Static and/or dynamic disorder will produce local configurations with much lower symmetry. It is difficult to deduce from the time- and space-averaged picture the local atomic arrangements. Unravelling atomic disorder very often requires independent information from techniques which can probe local arrangements. By combining spectroscopic (see section 4) and nuclear magnetic resonance (see section 5) with high-resolution diffraction data, a three-dimensional picture of the local atomic arrangements can be drawn.

Certainly the most useful crystallographic experiment on ice-Ih is performed with neutron radiation. Neutrons interact strongly with hydrogen, deuterium and oxygen atoms. The scattering power in the neutron case is a constant as a function of the scattering angle and similar for all three elements, whereas in the X-ray case it is proportional to the number of electrons and decreases with increasing scattering angle. The neutron scattering lengths [2] are $f_H = -3.74 \times 10^{-15}$ m, $f_D = 6.67 \times 10^{-15}$ m and $f_O = 5.81 \times 10^{-15}$ m. X-ray experiments are much less informative and provide useful data on the lattice constants and oxygen atoms only.

There is a slight complication in neutron scattering for atoms like hydrogen and deuterium, which have a nuclear spin. In this case the scattering depends on the relative orientation of the neutron spin and the spin

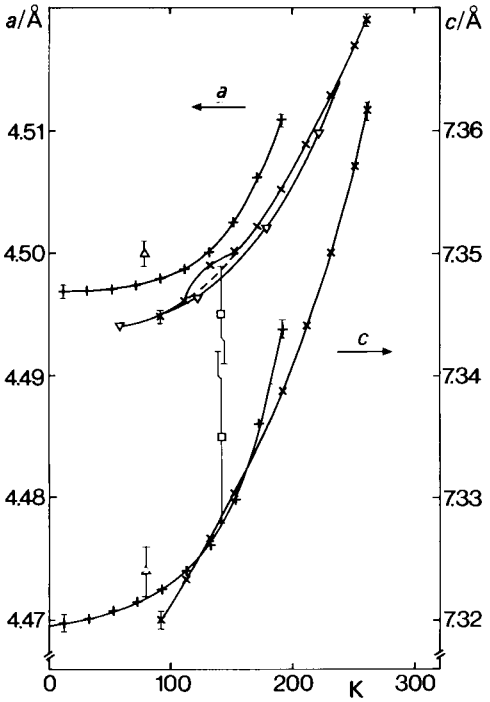

Figure 1. Lattice constants of ice-Ih: x, from La Placa and Post [4]; +, from Brill and Tippe [5]; and ▽, from Haltenorth [6]; all for H_2O. Single values are for D_2O: □, from Blackman and Lisgarten [7], and △, from Arnold *et al.* [8]. The lines are drawn as guides to the eye only. The error bars are plotted only at the lowest and highest temperature for each set.

of the nucleus. The orientation of the nuclear spin is different from atom to atom and thus also the interaction with neutrons. The spin incoherence gives rise to diffuse scattering, resulting in a considerably increased background intensity. This effect is weak in D_2O, but very strong in H_2O. However, in single-crystal neutral diffraction even the higher incoherent scattering cross-section of hydrogen is no serious problem, since the peak-to-background ratio for a Bragg peak is sufficiently high and since the incoherent scattering processes may be described as an absorption-like phenomenon, which is readily corrected for. Powder diffraction with its lower peak-to-background ratio suffers much from the strong incoherent scattering of hydrogen. Therefore neutron powder work is almost exclusively done on D_2O ices.

2.1. *The Lattice Constants*

The high resolution of X-ray powder diffractometers in principle allows the precise and accurate determination of the lattice constants in ice-Ih. Unfortunately there is still a considerable amount of disagreement about these basic quantities. The available data are plotted in figure 1. There are

Table 1. *Adopted† lattice constants of normal and heavy ice-Ih*

	H_2O (Å)		D_2O (Å)	
T(K)	a	c	a	c
60	4.4940(10)	7.318(2)	4.500_5(5)	7.329(8)
123	4.4962(10)	7.330(2)	4.503(5)	7.333(8)
223	4.5098(10)	7.347(2)	4.516(5)	7.351(8)

† The values for a_{H_2O} are taken from Haltenorth [6] and for c_{H_2O} mainly from La Placa & Post [4]. Note that Haltenorth does not give c_{H_2O}. Note further that a_{H_2O} agrees quite well in both references. Since in powder work the ratio of c/a is always more accurate than the individual lattice constants, we use the ratio from references La Placa and Post [4] and Brill and Tippe [5] to deduce c_{H_2O}. The lattice constants of heavy ice were deduced by combining some scattered single observations and the isotopic difference established in Lonsdale [3]. The estimated absolute errors obtained from Haltenorth [6] and the scatter in the data are quoted in brackets. All interatomic distances and angles calculated from crystallographic data and quoted in the following tables are based on these lattice constants.

indications that the lattice constants of H_2O and D_2O are different. Slightly larger volumes for heavy ice were already noticed in a critical review [3] of the early crystallographic data. Unfortunately, a more recent systematic study of lattice constants in heavy ice has not been performed. In normal ice-Ih anomalies along the a-direction were found near 120 K [4]. However, a re-examination [5] did not confirm this feature. Probably the most accurate study on the a lattice constant in H_2O was never published [6]. In general the internal agreement is rather poor by today's standards, and to obtain good estimates for D_2O is almost impossible in view of the widely scattered data points obtained at varying temperatures. For want of better measurements and in the balance of evidence, the lattice constants given in table 1 have been adopted in the following discussion. One should mention that the experimental scatter could be due to some real effect, e.g. inclusion of impurities, the size of crystallites, or even ageing effects, repeatedly invoked to explain discrepancies in other bulk measurements on ice-Ih. (See, for example [9], [10].)

2.2. *The Atomic Probability Density*

Diffraction data, or more accurately the intensities of the Bragg reflections observed at the nodes of the reciprocal lattice, carry information on the geometric arrangement of the atoms in a crystal. The intensity of a Bragg reflection, I_B, is proportional to the norm square, $F(Q)\cdot F(Q)^*$, of the structure amplitude $F(\boldsymbol{Q})$. The structure amplitude is given as

$$F(\boldsymbol{Q}) = \sum_n f_n \exp(\mathrm{i}\boldsymbol{r}_n\cdot\boldsymbol{Q})\cdot W(\boldsymbol{Q}) \qquad (2.1)$$

where $\boldsymbol{Q} = 2\pi(h\boldsymbol{a}^* + k\boldsymbol{b}^* + l\boldsymbol{c}^*)$ with h, k, l the Miller indices and $\boldsymbol{a}^*$, $\boldsymbol{b}^*$, $\boldsymbol{c}^*$ the reciprocal lattice constants. The position of atom n is described by $\boldsymbol{r}_n = x\boldsymbol{a} + y\boldsymbol{b} + z\boldsymbol{c}$ with x, y and z the fractional atomic coordinates and $\boldsymbol{a}$, $\boldsymbol{b}$, $\boldsymbol{c}$ the lattice constants. The individual atomic scattering power is dependent on the atomic scattering factor f_n. Atomic thermal motion reduces the measured intensities. In the harmonic approximation the weakening is given by the harmonic temperature factor

$$W(\boldsymbol{Q})_{\text{har}} = \exp\left[(2\pi)^{-2}(\boldsymbol{Q}^{\text{T}} \cdot \boldsymbol{\beta} \cdot \boldsymbol{Q})\right] \tag{2.2}$$

with the symmetric tensor $\boldsymbol{\beta}$ describing the anisotropy of the mean-square displacements and $\boldsymbol{Q}^{\text{T}}$ the transpose of the scattering vector $\mathbf{Q}$. Anharmonicity of the thermal motions or unresolved atomic disorder may occur and necessitate a more general temperature factor expression. [11] One very powerful generalized expression is based on the quasi-momentum expansion of the harmonic temperature factor

$$W(\boldsymbol{Q})_{gnrl} = W(\boldsymbol{Q})_{\text{har}} \cdot (1 - \tfrac{1}{6}\text{i}\gamma \cdot \boldsymbol{Q}^3 + \tfrac{1}{24}\delta \cdot \boldsymbol{Q}^4 + \ldots) \tag{2.3}$$

where γ and δ are the quasi-moment tensors of ranks 3 and 4 respectively.

The atomic positions, the harmonic and anharmonic thermal parameters are determined from the intensities by a least-squares procedure. The resulting atomic probability density function (*PDF*) centred at the refined atomic positions is calculated from the derived parameters as

$$PDF(\boldsymbol{u})_{\text{har}} = \text{Det}\, P^{\frac{1}{2}}[(2\pi)^{-\frac{3}{2}} \exp\left(-\tfrac{1}{2}\boldsymbol{u}^{\text{T}} \cdot \text{P} \cdot \boldsymbol{u}\right)] \tag{2.4}$$

with $\mathbf{P} = 2\pi^2\boldsymbol{\beta}^{-1}$, where $\boldsymbol{\beta}$ is the anisotropic mean-square-displacement tensor; $\mathbf{u}$ and $\mathbf{u}^{\text{T}}$ are the displacement vector and its transpose, respectively.

In the generalized form this trivariate *PDF* reads

$$PDF(\boldsymbol{u})_{gnrl} = PDF(\boldsymbol{u})_{\text{har}} \cdot \left(1 + \frac{1}{3!}\gamma \cdot H_3(\boldsymbol{u}) + \frac{1}{4!}\delta \cdot H_4(\boldsymbol{u}) + \ldots\right) \tag{2.5}$$

with H_3 and H_4 being the Hermite polynomials of order 3 and 4. The higher order terms in brackets describe the anharmonic deformations of the harmonic (Gaussian) probability density. The calculated anharmonic deformation densities have been found to be very useful in detecting weak atomic disorder [11].

For an atom in a perfectly harmonic potential the mean and equilibrium positions are identical, while they are different in general in the case of anharmonicity. Employing the harmonic description (equations (2.1) and (2.2)) for anharmonic atomic potentials is certainly not adequate and corrections have to be applied to obtain the equilibrium positions (see equation (4.32)). By employing the generalized expressions (equations (2.3) and (2.5)) both equilibrium and mean positions are obtained. The accuracy of their determination is only limited by the adequacy of the chosen mathematical description, and the quasi-momentum expansion underlying

equations (2.3) and (2.5) has proven to be adequate even in the case of strong anharmonicities [11]. Moreover, the generalized expressions describe not only anharmonic modifications of atomic densities, but also their curvilinear shape due to librational motions. Again corrections have to be made when harmonic models are used. In the case of librations of hydrogen or deuterium it is generally assumed that they 'ride' on the oxygen atom. The riding correction is given by [12]

$$\Delta r_{\mathrm{H(D)}} = r_{\mathrm{O-H(D)}} \langle \phi^2 \rangle \tag{2.6}$$

where $\langle \phi^2 \rangle$ is the mean-square angular displacement of librational motion. The best estimate of $\langle \phi^2 \rangle$ in disordered systems like ice-Ih is obtained from spectroscopy (see section 4).

2.3. *The Averaged Structure of Ice-Ih*

The time- and space-averaged structure of ice-Ih can be obtained with high precision and accuracy from neutron diffraction experiments, preferably on single crystals. The symmetry and unit cell of the averaged structures were correctly described by Barnes [13] from single-crystal X-ray data. Ice-Ih crystallizes in the hexagonal space group $P6_3/mmc$ with oxygen atoms placed at the four-fold position [14] (f): $\pm(\frac{1}{3}, \frac{2}{3}, z; \frac{2}{3}, \frac{1}{2}+z)$. The oxygen framework forms a very open structure and is shown in figure 2. The positions of the hydrogen atoms were first established by Wollan *et al.* [15] from neutron power data. Hydrogen or deuterium atoms are distributed over two sites, one four-fold position (f) and one twelve-fold position (k) [14]: $\pm(x, 2x, z; x, \bar{x}, z; 2\bar{x}, \bar{x}, z; x, 2x, \frac{1}{2}-z; x, \bar{x}, \frac{1}{2}-z; 2\bar{x}, \bar{x}, \frac{1}{2}-z)$. The averaged occupancy on these sites is 50% in agreement with Pauling's [16] half-hydrogen model. The atomic arrangement is shown in figure 3.

In a single-crystal neutron diffraction study performed at 123 and 223 K, Peterson and Levy [17] have provided a full description of the averaged structure of ice-Ih. The anisotropic atomic mean-square displacements were obtained and analysed. Pauling's half-hydrogen model was fully confirmed and the mean-square displacements of deuterium relative to oxygen essentially along the bond directions were found to be in agreement with spectroscopy. Later Chidambaram [18] proposed a bent hydrogen-bond model; displacing the hydrogen atoms from the *c*-axis and thus allowing the water angle to be preserved in ice-Ih, gave as good an agreement with Peterson and Levy's [17] data as the simple half-hydrogen model. Chamberlain *et al.* [19] studied doped H_2O ice at 77 K and essentially confirmed the validity of the half-hydrogen model for H_2O at low temperatures. Recently Kuhs and Lehmann [20–23] performed a series of high-resolution neutron diffraction studies on H_2O and D_2O ice-Ih in order to clarify some questions concerned with the molecular geometry. Doubts were raised (for example [24]) as to the correctness of the long O–H bond found in the earlier crystallographic work

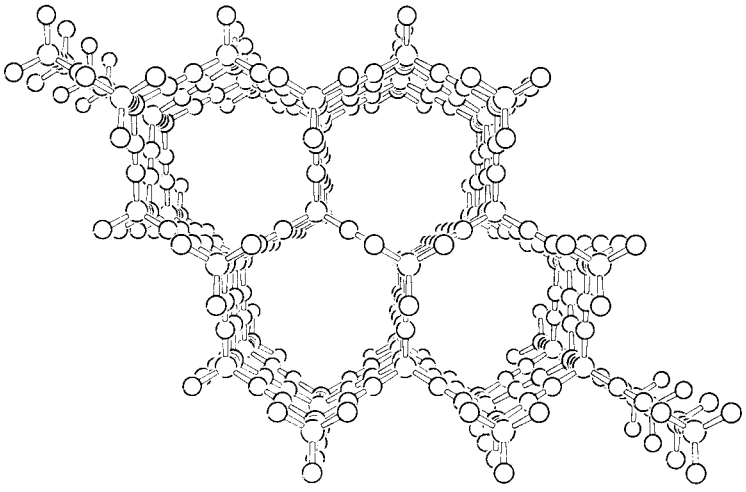

(a)

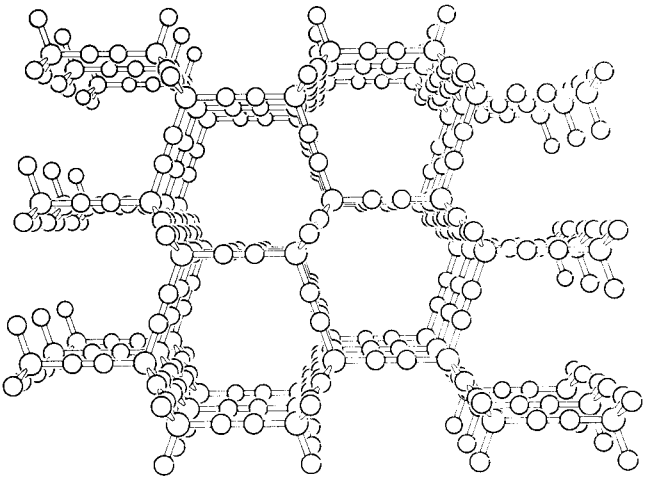

(b)

Figure 2. Framework of the oxygen atoms viewed along the *c*-axis (a) and along the *a*-axis (b) showing the open structure of ice-Ih.

[17, 19] and the validity of the bent hydrogen-bond model [18] was awaiting experimental proof. Data on H_2O and D_2O ice-Ih were collected at 60, 123 and 223 K and corrections for absorption (H_2O only) and first-order thermal diffuse scattering applied. Extinction was corrected in a first structure refinement stage. After averaging of equivalent reflections, the final structure

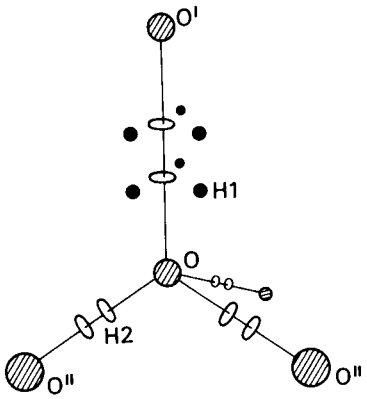

Figure 3. Averaged atomic arrangement in one oxygen tetrahedron of ice-Ih. The hydrogen positions are half occupied ('half-hydrogen model'). The bent hydrogen model [18] is indicated as a further splitting perpendicular to the *c*-axis.

Table 2. *Averaged molecular geometry in ice-Ih*

	H_2O			D_2O		
	60 K†	123 K†	223 K†	60 K†	123 K†	223 K‡
O–H1	1.005(2)	1.009(2)	1.000(4)	1.003(1)	1.002(1)	1.000(9)
O–H2	1.005(1)	1.005(1)	0.997(2)	0.999_5(1)	1.001(1)	1.007(5)
H1–H2	1.638(3)	1.643(3)	1.632(5)	1.633(1)	1.634(1)	1.635(12)
H2–H2	1.645(2)	1.641(2)	1.628(4)	1.634(2)	1.636(1)	1.648(9)
H1–O–H2	109.15(13)	109.42(14)	109.52(24)	109.31(6)	109.30(6)	109.10(30)
H2–O–H2	109.79(13)	109.53(14)	109.43(24)	109.63(6)	109.65(6)	109.86(26)

† Data from Kuhs and Lehmann [23].
‡ Data from Peterson and Levy [17].

refinements were performed. Tables 2 to 4 give the results obtained for the half-hydrogen model with an harmonic description of thermal motions (equations (2.2) and (2.4)). Although oxygen disorder and bent hydrogen bonds have not been included at this stage, valuable information is gained from this very global averaging over all local configurations. Several points emerge from an intercomparison of the results as a function of temperature and composition. As expected, the intermolecular distances increase in H_2O and D_2O as a function of temperature, while the change in the averaged intramolecular geometry is barely significant. The slight differences in bond length in H_2O and D_2O are due to the different magnitudes of stretch anharmonicity and libration. The intermolecular distances along and oblique

Table 3. *Averaged hydrogen-bond geometry in ice-Ih*

	H_2O			D_2O		
	60 K†	123 K†	223 K†	60 K†	123 K†	223 K‡
O–O′	2.748(1)	2.752(1)	2.760(1)	$2.754_5(1)$	2.755(1)	2.752(8)
O–O″	2.749(1)	2.752(1)	2.759(2)	2.753(1)	2.755(1)	2.765(1)
O–H1	1.743(2)	1.743(1)	1.758(3)	1.752(1)	1.753(1)	1.751(10)
O–H2	1.744(1)	1.747(1)	1.763(2)	1.754(1)	1.754(1)	1.759(6)
O–H1–O′	180.00	180.00	180.00	180.00	180.00	180.00
O′–H2–O″	179.73(20)	179.93(21)	179.76(37)	179.99(9)	179.96(10)	176.8(2)
O′–O–O″	109.32(2)	109.37(2)	109.36(4)	109.30(1)	109.32(1)	109.55(15)
O″–O–O″	109.62(2)	109.57(2)	109.58(4)	109.64(1)	109.62(1)	109.40(2)

† Data from Kuhs and Lehmann [23].
‡ Data from Peterson and Levy [17].

Table 4. *Total† atomic mean-square displacements in ice-Ih*

	H_2O			D_2O		
	60 K‡	123 K‡	223 K‡	60 K‡	123 K‡	223 K§
O//c	0.01466(14)	0.02467(18)	0.04415(50)	0.01352(9)	0.02353(12)	0.02900(215)
O⊥c	0.01465(8)	0.02486(11)	0.04531(28)	0.01399(5)	0.02354(9)	0.03027(279)
H1//c	0.01904(49)	0.02812(58)	0.04906(175)	0.01605(20)	0.02495(22)	0.03762(355)
H1⊥c	0.03239(35)	0.04171(42)	0.05828(80)	0.02593(14)	0.03457(16)	0.04091(279)
H2//O–O″	0.01913(34)	0.02870(45)	0.04767(134)	0.01662(13)	0.02570(15)	0.03356(320)
H2//a	0.03262(48)	0.04161(57)	0.05830(103)	0.02580(17)	0.03431(19)	0.04889(576)
H2⊥a	0.03234(48)	0.04125(55)	0.05893(115)	0.02568(16)	0.03409(19)	0.04040(424)

† The mean-square displacements quoted include possible disorder displacements.
‡ Data from Kuhs and Lehmann [23].
§ Data on D_2O at 223 K are taken from Peterson and Levy [17]. Since a correction for thermal diffuse scattering was not made, the values quoted are considerably too low and cannot be used for a more detailed analysis.